Brazilian Journal of Microbiology (2023) 54:1341–1350
https://doi.org/10.1007/s42770-023-01050-x

BACTERIAL AND FUNGAL PATHOGENESIS - RESEARCH PAPER

Effect of green Fe_2O_3 nanoparticles in controlling *Fusarium* fruit rot disease of loquat in Pakistan

Faryal Niazi[1] · Musrat Ali[1] · Urooj Haroon[1] · Farhana[1] · Asif Kamal[1] · Taskeen Rashid[1] · Fareeha Anwar[1] · Rabia Nawab[1] · Hassan Javed Chaudhary[1] · Muhammad Farooq Hussain Munis[1]

Received: 16 July 2022 / Accepted: 24 June 2023 / Published online: 4 July 2023

Abstract

The subtropical fruit known as the loquat is prized for both its flavour and its health benefits. The perishable nature of loquat makes it vulnerable to several biotic and abiotic stressors. During the previous growing season (March–April 2021), loquat in Islamabad showed signs of fruit rot. Loquat fruits bearing fruit rot symptoms were collected, and the pathogen that was causing the disease isolated and identified using its morphology, microscopic visualisation, and rRNA sequence. The pathogen that was isolated was identified as *Fusarium oxysporum*. Green synthesized metallic iron oxide nanoparticles (Fe_2O_3 NPs) were employed to treat fruit rot disease. Iron oxide nanoparticles were synthesized using a leaf extract of the *Calotropis procera*. Characterization of NPs was performed by different modern techniques. Fourier transform infrared spectroscopy (FTIR) determined the existence of stabilizing and reducing compounds like phenol, carbonyl compounds, and nitro compounds, on the surface of Fe_2O_3 NPs. X-ray diffraction (XRD) explained the crystalline nature and average size (~49 nm) of Fe_2O_3 NPs. Energy dispersive X-ray (EDX) exhibited Fe and O peaks, and scanning electron microscopy (SEM) confirmed the smaller size and spherical shape of Fe_2O_3 NPs. Following both in vitro and in vivo approaches, the antifungal potential of Fe_2O_3 NPs was determined, at different concentrations. The results of both in vitro and in vivo analyses depicted that the maximum fungal growth inhibition was observed at concentration of 1.0 mg/mL of Fe_2O_3 NPs. Successful mycelial growth inhibition and significantly reduced disease incidence suggest the future application of Fe_2O_3 NPs as bio fungicides to control fruit rot disease of loquat.

Keywords *Fusarium oxysporum* · Fruit rot · Green synthesis · *Calotropis procera* · Fe_2O_3 NPs · NPs characterization

Introduction

Loquat (*Eriobotrya japonica* Lindl.) is a member of family Rosaceae, subfamily Pomoideae, and it is mostly cultivated in subtropical areas [1]. Loquat tree has medicinal and ornamental importance. It is used to treat respiratory disorders, infection, and cancer [2, 3]. Major loquat producing countries are China, Pakistan, Mauritius Island, Japan, Reunion Island, India, and Mediteranean countries [4–6]. Approximate fruit production of loquat is 549,220 tonnes, worldwide. China is the major fruit producing country followed by Spain, Japan, India, and Pakistan [7, 8]. In Pakistan, loquat is grown in Murree, Hasan Abdal, Mardan, Tret, Kalar Kahar, Wah, Haripur, Sargodha, Choa Saiden Shah, Kasur, and Chhattar [9]. In Pakistan, Punjab and Khyber Pakhtunkhwa are the major loquat producing provinces [10].

Fungi are major biotic factors to causes 50% yield losses in fruit crops. Approximately one third of all food crops are destroyed by fungal pathogens [11]. About 248 species of fungi have been reported to cause diseases of *E. japonica* [12]. *Colletotrichum gloeosporioides* and *Colletotrichum truncatum* have been reported to cause pre-harvest and post-harvest diseases of loquat [13, 14]. Previous studies have described fungal diseases of loquat including anthracnose [15], fruit rot by *Colletotrichum* species [16], fruit rot by *Lasiodiplodia theobromae* [17, 18], circular brown leaf

Responsible Editor: Admir Giachini

✉ Muhammad Farooq Hussain Munis
munis@qau.edu.pk

[1] Department of Plant Sciences, Faculty of Biological Sciences, Quaid-i-Azam University, Islamabad 45230, Pakistan

spot [19], *Fusarium* fruit rot [17], and scab by *Fusicladium eriobotryae* [20–22]. In Pakistan, few major fungi including *Diplodia seriata* [23], *Fusarium solani* [17], *C. gloeosporioides* [24], *Curvularia lunata* [25], and *Alternaria mali* [26] have been reported to cause diseases on different parts of loquat tree.

Use of chemical fungicide is very common in different parts of the world [27]. In Pakistan, approximately 108 types of insecticides are being used [28]. Fungicides have possible side effects, and they have been reported to affect human health [29]. Due to these health risks, scientists are working on environment-friendly disease control technologies for controlling post-harvest fruit disease [30, 31]. Nowadays, there is too much attention for alternatives of chemical fungicides and development of biological control measures against plant diseases [32]. Due to their biological origin, bio fungicides have minimal toxicity and increased resistance against diseases, and they are cheaper [33].

Nanotechnology is inspiring weapon against many factors that threaten plant health [34]. Green synthesis of nanoparticles involving the use of plants to synthesize metallic nanoparticles is safe and has environment friendly approach. To synthesize nanoparticles, different plant parts such as stem, seeds, leaves, roots, and fruits are being used. All these parts contain phytochemicals that have stabilizing and reducing abilities [35]. The aqueous leaf extract of *C. procera* has been used to synthesize nanoparticles. Antimicrobial potential of *C. procera* is well-documented [36]. To overcome drawbacks of classical hazardous disease-control methods, use of plants to synthesize nanoparticles is a novel approach, as the phytochemicals of plants act as capping and reducing agents [37]. Efficient application of Fe_2O_3 NPs in controlling fruit rot diseases has been reported earlier [38]. Iron oxide nanoparticles synthesized in aqueous leaf extract of *Calotropis procera* has been reported to control fruit rot of cherry [39]. Iron oxide NPs have also diminished the rot of apple [40].

The goal of this study was to synthesize iron oxide nanoparticles using the aqueous leaf extract of *C. procera* that could be used to treat post-harvest pathogen of loquat.

Materials and methods

Collection of diseased fruit

During the months of March–April 2021, field surveys were conducted, and diseased loquat samples were collected from the orchards of Quaid-i-Azam University Islamabad. Collected fruits were transferred to the lab in sterile polythene bags for further analyses [39].

Isolation of pathogen

Loquat fruit surface sterilization was done with 1% sodium hypochlorite solution (1 mL of sodium hypochloride was dissolved in 99 mL of distilled water) and then washed with distilled water for 2 min before isolation of causative agent. With sterilized blade, segments of diseased fruits were cut from edges and put on potato dextrose agar (PDA) media plates. Petri plates were sealed using parafilm and were kept in an incubator at 25 ± 2 °C. After 5 to 7 days, fungus morphology was observed by observing the colony growth, color, and its pattern from front and backside of the plate [40].

In vivo pathogenicity test

Pathogenicity was confirmed by following Koch's postulates. Mycelia of 7-day-old fungus were transferred to Czapek broth media and placed in shaking incubator at 25 ± 2 °C. After achieving desired concentration of conidia suspension (10^6 conidia/ mL), broth culture was filtered to remove mycelia. To infect healthy loquat fruit, wounded sterile needle was used, and 5 µL conidial suspension was injected into three randomly selected fruit. Control fruits were injected with sterile distilled water. To protect all treated fruits, muslin cloth was used and kept in an incubator at 25 ± 2 °C. After 1 week, symptoms of disease with earlier field symptoms were compared. Pathogen was re-isolated by culturing on PDA media for 5–7 days at 25 ± 2 °C [39].

Microscopic identification

For identification, hyphae along with reproductive structures of isolated fungus were analyzed under light microscope. Slides were prepared using lactophenol blue [41]. Drop of lactophenol blue was placed in the center of slide, and growing mycelium was mounted on slides. By avoiding air bubbles, cover slip was placed, and slide was observed under microscope at ×100 magnification to examine spores, hyphae, and other pathogenic characteristics [42].

Molecular characterization and phylogenetic analysis

For genetic identification, rDNA of isolated fungus was amplified using specific small subunit ribosomal RNA primers. CTAB method was used for the extraction of fungal DNA [43]. The fungal mycelia (50 mg) were scraped from 10-day-old PDA cultures, manually ground in 1.5 mL of microfuge tubes with micro pestle adding 500 µL of pre-warmed (60 °C) TES lysis buffer (100 mM Tris pH 8.0; 10 mM EDTA pH 8.0; 2% SDS) of proteinase K

that was added to the ground material, incubated in 60 °C for 60 min. One hundred forty microliter of 5M NaCl and 64 µL of 10% (w/v) of CTAB were added to the suspension incubated at 65 °C for 10 min. DNAs were extracted by adding equal volume of chloroform: isoamylalcohol (24:1) centrifuged at 14000 × g/10 min. DNA was precipitated by adding 0.6 volume of cold isopropanol and 0.1 volume of 3M sodium acetate pH 5.2, centrifuged, and washed twice with 70% ethanol suspended in 100 µL of TE (10 mM Tris pH 8.0; 1 mM EDTA pH 8.0). RNA was digested by adding 10 mg/mL of RNAse A and incubating at 37 °C for 45 min and stored at −20 °C for further use. For the amplification of rRNA, in polymerase chain reaction (PCR), ITS1 forward (TCCGTAGGTGAACCTGCG G) and ITS4 reverse (TCCTCCGCTTATTGATATGC) primers were used [44]. Reaction mixture contains 0.5 µL of dNTPs, 1.5 µL of *Taq* DNA polymerase, 5 µL of 10× polymerase buffer, 1 µL of genomic DNA, and 1 µL of each primer. PCR reaction temperature was 94 °C for 4 min, followed by 35 cycles of 94 °C for 40 s, 58 °C for 40 s, and 72 °C for 40 s. Sequencing of amplified PCR product was done and subjected to BLAST analysis on NCBI database. MEGA 7 with maximum likelihood method with 1000 bootstrap was used for phylogenetic analysis [45].

Preparation of leaf extract

To prepare extract, fresh leaves of *Calotropis procera* were washed and shade dried for 1 week. Leaves were ground into fine powder. *C. procera* extract was prepared by mixing of 30 g of powder into 300 mL of de-ionized water and boiled for 5 to 10 min. Solution was warmed up in water bath at temperature of 80 °C for 30 min. Extract was permissible to cool down and then filtered through muslin cloth. Further filtration was performed using Whatman filter paper and kept at 4 °C for storage [39].

Calotropis procera-mediated synthesis of iron nanoparticles

For the preparation of Fe_2O_3 NPs, 1 mM $FeCl_3$ solution was prepared and added into *C. procera* extract in 1:1 ratio. Heating temperature of hot plate for blend was 80 °C for 120 min, until the color was changed. Color change was the indication of reduction process of Fe_2O_3 NPs. Mixture was centrifuged for 10 min at 6000 rpm, and the pellet was washed with de-ionized water. Pellet was dried in an incubator for 3 to 4 h at 100 °C. Crystalline form of Fe_2O_3 NPs was obtained by calcination at 500 °C for 2 to 3 h. The synthesized nanoparticles were characterized before their antifungal activity analyses [39].

Characterization of nanoparticles

Fe_2O_3 NPs were characterized by the different laboratory techniques [46].

FTIR spectroscopy

Fourier transform infrared spectroscopy (FTIR) was used to determine the nature and types of functional groups associated with iron nanoparticles, in the range of 400 to 4000 cm^{-1} with resolution power of $4cm^{-10}$. KBr pellet method was adopted to prepare sample by enveloping 10 mg of nanoparticles in 100 mg of KBr pellet.

XRD

To understand the nature and size of nanoparticles, X-ray diffraction (XRD) spectroscopy was used. Size of synthesized Fe_2O_3 NPs was assessed by the following Scherrer equation:

$$D = K\lambda/\beta\cos\theta$$

D is the crystalline size, shape factor is K, λ is the wavelength of X-ray, ß is the full width at half-maximum of radians, and θ is angle of diffraction.

SEM-EDX characterization

Scanning electron microscopy (SEM) was used to see the morphology of NPs. There was use of energy dispersive X-ray spectroscopy (EDX) to reveal elemental composition of Fe_2O_3 NPs. Fe and O peaks were observed in X-ray spectra.

In vitro antifungal assay of Fe_2O_3 NPs

Fe_2O_3 NP fungicidal activity against *F. oxysporum* was tested by poisoned food technique [47]. Five concentrations of Fe_2O_3 NPs (0.1, 0.25, 0.50, 0.75, and 1 mg/ ml) were mixed with PDA media. Fungal discs (5 mm) were positioned in the middle of each Petri plate. One Petri plate with no Fe_2O_3 NPs was used as a control. Plates were kept in an incubator at 25 °C. Percentage inhibitions and diameters of fungal mycelia were measured at regular intervals in 7 days. Following formula was used to calculate inhibition percentage of fungal growth:

$$\text{Growth inhibition percentage} = (C - T)/C \times 100$$

where *C* is the growth in the control and *T* is the sample mycelial growth [36].

In vivo antifungal activity analysis of Fe_2O_3 NPs

For the control of disease on loquat fruit, Fe_2O_3 NPs were used, following "detached fruit inoculation method" [48]. For this purpose, 18 fruits were surface sterilized, wounded with needle, and inoculated with fungus. After inoculation of fungus, Fe_2O_3 NPs were applied in five different concentrations (0.1, 0.25, 0.50, 0.75, and 1.0 mg/mL). Each concentration was applied on three inoculated fruit, and all samples were kept at 25 °C in an incubator. Lesions on fruit were observed, and area of lesion was measured in regular intervals of 72 h of treatment.

Statistical analysis

Experimental data was statistically analyzed by following one-way ANOVA. The significance of difference between treatments was tested by least significance difference (LSD) post hoc test ($\alpha = 0.05$). All data expressed as mean ± standard error.

Results

Morphological and microscopic identification of pathogen

Diseased samples were collected (Fig. 1a), and after isolation from diseased fruit, the color of aerial mycelium was faded white, which later changed to purplish blue color (Fig. 1b). Mycelial color, on the backside of petri plates, was light yellow (Fig. 1c). Macro conidial septation was observed under microscope (Fig. 1d).

Abundant chlamydospores were produced. These all-surface pattern and microscopic examinations demonstrated this pathogen as *F. oxysporum* [17].

In vivo pathogenicity test

Koch's postulates validated pathogenicity of isolated *F. oxysporum*. After 3 days of inoculation of healthy fruit, light brown disease circles were observed (Fig. 1e), which enlarged in size, later (Fig. 1f). These disease symptoms were similar to the symptoms of initially collected diseased fruit. Fungus was re-isolated and showed similar growth pattern to inoculated fungus (Fig. 1g, h). Based on these findings, *F. oxysporum* was demonstrated as causal agent of loquat fruit rot disease.

Molecular identification and phylogenetic analysis of isolated fungus

Isolated fungus sequence was 100% similar with *F. oxysporum* strain FO_99 (Accession no. MT649536.1). The sequence was submitted in NCBI database with accession number OL744437. Maximum likelihood method was successfully used to construct phylogenetic tree, which showed that the presence of obtained sequence is the same clade with *F. oxysporum* (Fig. 2). It also confirmed the evolutionary relationship of isolated fungus with *F. oxysporum*.

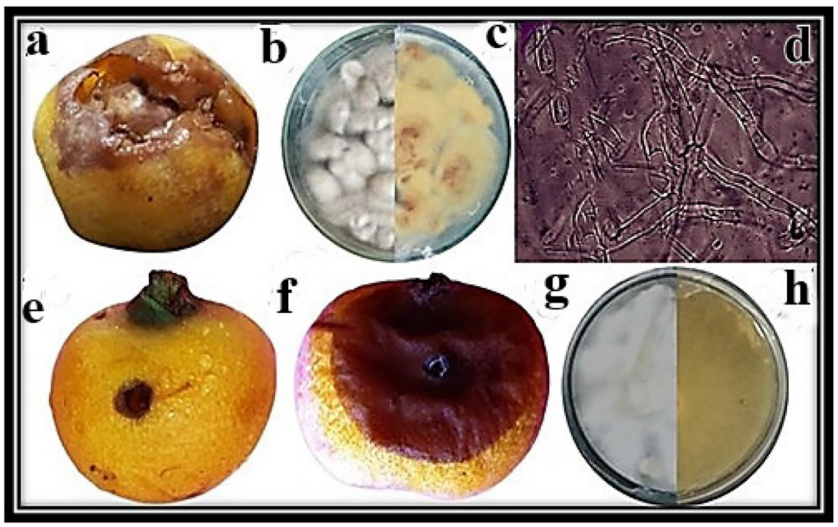

Fig. 1 Fruit rot symptoms were observed on loquat fruit (**a**). Disease-causing pathogen was isolated and observed from the front side (**b**) and back side of the Petri plates (**c**). Microscopic observation of fungus was performed at ×40 magnification (**d**). Fungus was re-inoculated on healthy fruit, and disease symptoms were observed after 3 days (**e**) and 5 days post inoculation (**f**). Pathogen was re-isolated on PDA and observed from front side (**g**) and back side (**h**)

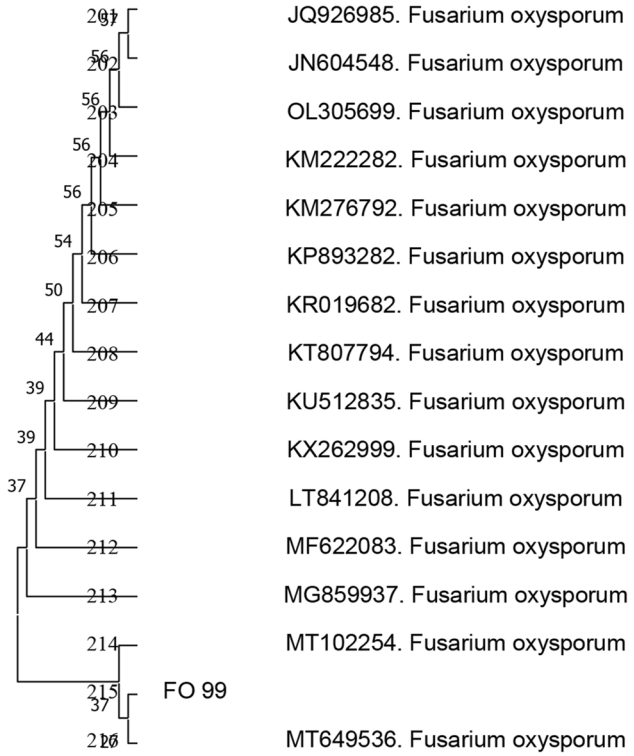

Fig. 2 Phylogenetic analysis of isolated pathogen with 15 related gene sequences from GenBank

Characterization of green synthesized Fe_2O_3 NPs

FTIR

FTIR spectra of Fe_2O_3 NPs showed different absorption band (Fig. 3). Absorption peak at 3414.48 cm^{-1} represented O-H stretching. Absorption peak at 1739.97 cm^{-1} showed C=O stretch of aldehyde group. Stretching vibrations at 1653.12 cm^{-1} described alkene group while 1599.47 cm^{-1} attributed polyphenols [49]. Stretching vibrations at 1558.83 cm^{-1} and 1506.56 cm^{-1} demonstrated nitro compounds (N-O). Peak at 1367.44 cm^{-1} signified S=O stretching of sulfonamide group. Peak at 1149.97 cm^{-1} indicated C-O stretching of aliphatic ether. Stretching vibrations of Fe-OFe were observed at 667 cm^{-1}, 512 cm^{-1}, and 433 cm^{-1} [14].

XRD

Crystalline structure of Fe_2O_3 NPs was described by XRD spectroscopy (Fig. 4). XRD pattern showed five notable peaks at 2θ angle between 10^0 and 80^0. Peaks were observed at 11^0, 15.8^0, 20.5^0, 30.7^0, and 43^0. The average size of nanoparticle was observed to be 49 nm. Sharp peaks revealed crystalline nature of Fe_2O_3 NPs. Crystalline nature of NPs is inclined by plant extract [43]. Other than these peaks, there were no other detectable peaks, which indicated the purity of sample. XRD pattern of Fe_2O_3 NPs was in accordance with previous studies [7].

SEM and EDX analyses

SEM analysis explored the surface of synthesized NPs (Fig. 5). From the micrographs, spherical shape of Fe_2O_3 NPs was observed. These NPs were present in a size range of 40 to 50 nm and confirmed the size of NPs, estimated from XRD spectra. Fe_2O_3 NPs were spherical in shape. Peaks of Fe and O in EDX confirmed the formation of NPs. Weight percentage of chlorine, iron, and oxygen was 45.67%, 43.06%, and 20.18%, respectively (Fig. 6).

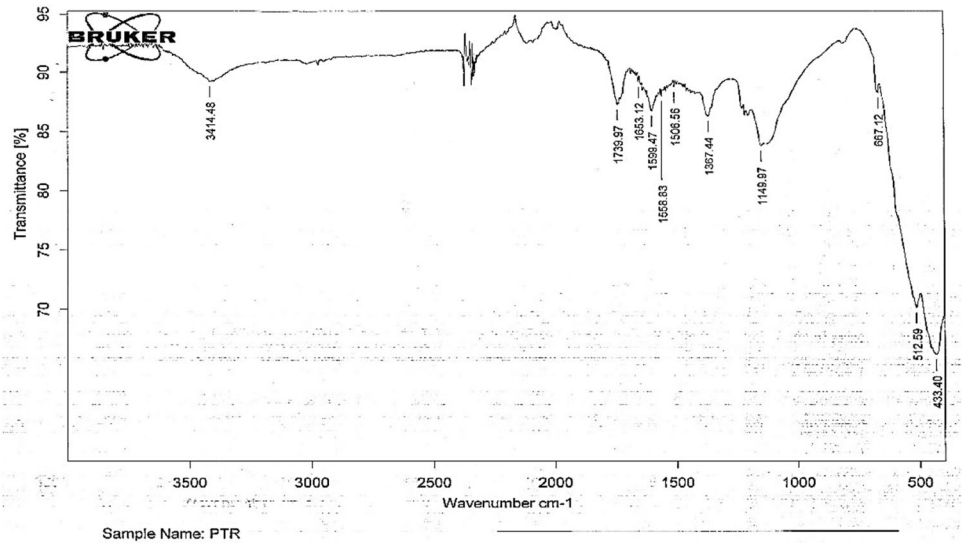

Fig. 3 FTIR spectrum of Fe_2O_3 NPs synthesized in the leaf extract of *C. procera*

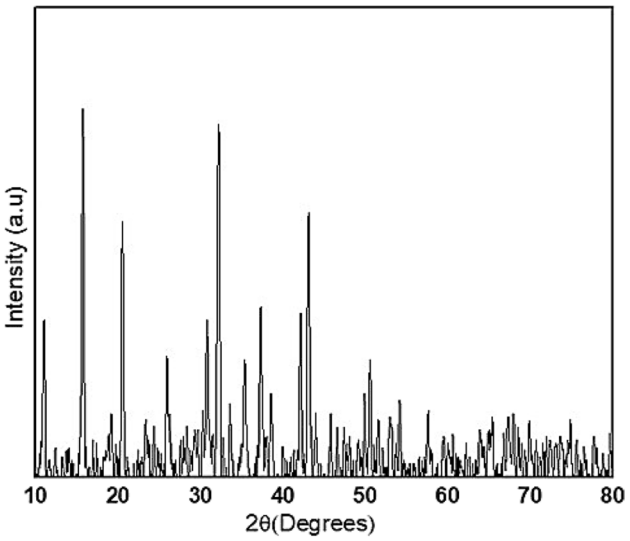

Fig. 4 XRD pattern of Fe_2O_3 NPs synthesized in the leaf extract of *C. procera*

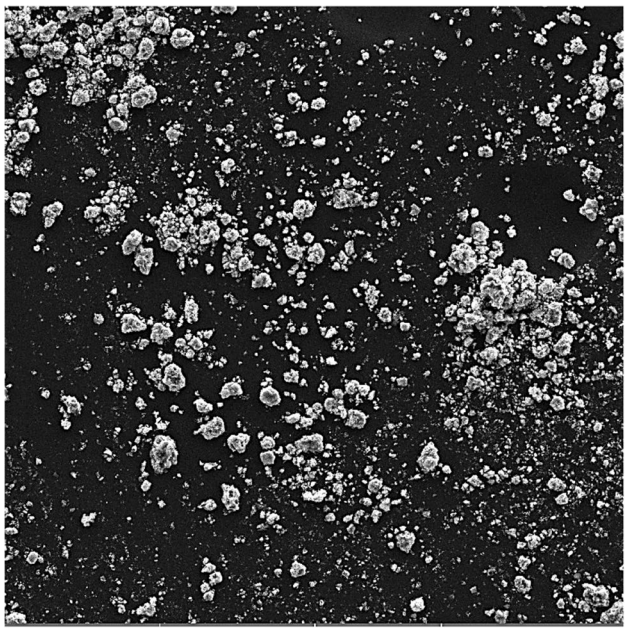

Fig. 5 SEM of Fe_2O_3 NPs synthesized in the leaf extract of *C. procera*

Antifungal activity of Fe_2O_3 NPs, in vitro

NPs of Fe_2O_3 showed maximum mycelial growth suppression (72%) at the concentration of 1 mg/mL. While growth inhibition at 0.75, 0.50, 0.25, and 0.1 mg/mL was 64.44%, 60%, 52%, and 37% (Table 1) (Fig. 7).

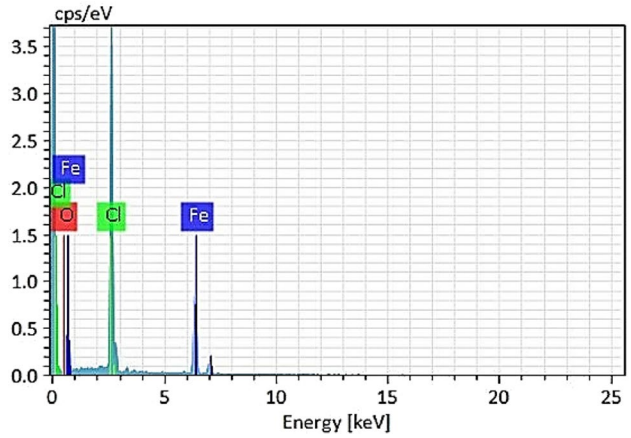

Fig. 6 Energy dispersive X-ray (EDX) spectroscopy of Fe_2O_3 NPs revealed the presence of Fe, Cl, and O

Table 1 Mycelial growth inhibition at different concentration of Fe_2O_3 NPs

Concentration mg/mL	Inhibition percentage
1.0	72.22 ± 1.0
0.75	64.44 ± 1.0
0.50	60.77 ± 0.5
0.25	52.22 ± 0.8
0.1	37.77 ± 1.2

Antifungal activity of Fe_2O_3 NPs, in vivo

In vivo antifungal activity analysis revealed the best disease control at concentration of 1.0 mg/mL of Fe_2O_3 NPs. All concentration of Fe_2O_3 NPs exhibited variable disease control (Fig. 8).

Discussion

Most frequent disease of loquat and other perishable fruits is fruit rot [15]. This work includes a thorough examination of the mycobiota linked to the fruit rot of loquat in Islamabad. To obtain pure colonies, the pathogen was isolated from rotten fruit segments and cultured on Petri plates. Utilizing morphological and molecular traits, fungal isolates were identified. Isolated fungus from loquat was identified as *F. oxysporum*. Microscopic observation revealed similar morphology, and macro conidial septation has been described earlier [50].

To control plant diseases, biocontrol efforts are being done for last few decades. Nanomaterials have gained popularity in the modern period as a result of their unique features and important applications in the food and agricultural industries [51]. The

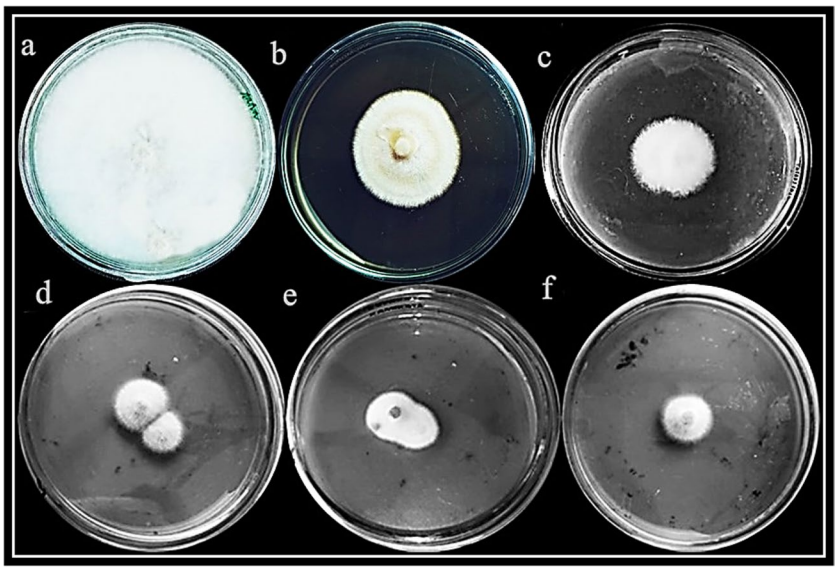

Fig. 7 Inhibitory effect of Fe_2O_3 NPs on *F. oxysporum* using five different concentrations of NPs. Fungus growth was observed in control (**a**) and at five concentrations of NPs including 0.1 mg/mL (**b**), 0.25 mg/mL (**c**), 0.50 mg/mL (**d**), 0.75 mg/mL (**e**), and 1.0 mg/mL (**f**)

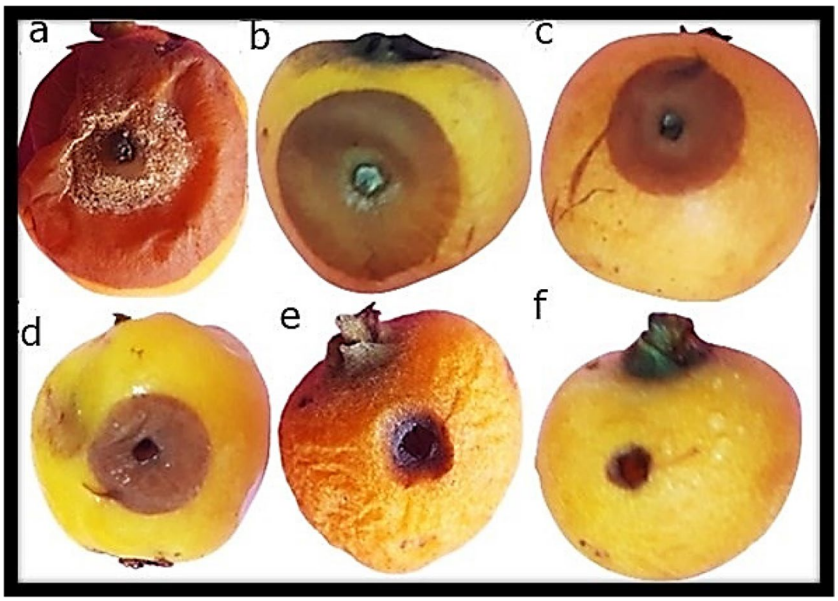

Fig. 8 Control of fruit rot disease using Fe_2O_3 NPs on loquat. Control fruit exhibited maximum disease (**a**). Variable fruit rot disease was observed at 0.1 mg/mL (**b**), 0.25 mg/mL (**c**), 0.50 mg/mL (**d**), 0.75 mg/mL (**e**), and 1.0 mg/mL (**f**) concentration of Fe_2O_3 NPs

manufacturing of nanoparticles has advanced greatly, and a wide range of biological agents, including bacteria and plants, are being exploited [52]. Use of plants to synthesize metallic nanoparticles is a more simple method, and many plant metabolites act as stabilizing and reducing agents [49].

In this study, *C. procera* was successfully used to synthesize iron oxide nanoparticles. Antifungal potential of *C. procera*-mediated NPs has been described earlier [39]. With the aid of FTIR, XRD, SEM, and EDX, iron oxide nanoparticle characterization was performed. Different functional groups were identified by FTIR spectrum. These functional groups consist of bioactive molecules. While reviewing FTIR spectra, amino groups were present, and they show the presence of proteins all around iron oxide NPs. Results affirmed that protein molecules are present in the extract, and they are able to function as stabilizing and reducing agent by attachment to iron oxide NPs, with the aid of free primary amino group [53]. Carboxylic groups help to bind on Fe surface [54]. XRD affirmed crystal nature and smaller size of NPs. Previous research has demonstrated that small size and crystalline structure of NPs provide them strong antimicrobial capabilities [40, 46].

SEM images revealed spherical shape of iron oxide NPs. Additionally, high surface area to volume ratio was observed that depicted that nanoparticles have a propensity to aggregate in suspension [55]. An EDX study

verified the elemental composition of the iron oxide nanoparticles' elemental makeup. Iron oxide nanoparticles' EDX spectrum pattern revealed narrow peaks that confirmed the crystalline structure of the iron nanoparticles [56]. The EDX spectra revealed the existence of iron peaks in two distinct regions. The culture filtrate may be responsible for the existence of additional organic substances like O and C [57]. Iron oxide NPs were synthesized using a precursor solution that contained the element chlorine [58].

In this study, different concentrations of iron oxide nanoparticles synthesized using *C. procera* (0.1, 0.25, 0.5, 0.75, and 1 mg/mg) were utilized to both in vitro and in vivo test to suppress the fungus that causes fruit rot disease in loquat. It was found that the antifungal activity increased with increasing NP concentration. NP application results in membrane disability of fungus, by producing active oxygen radical suppression of transporter genes and genotoxicity [59]. NPs affect morphological properties of fungal membrane like depolarization of membrane and permeability. This breakdown causes leakage of different substances like enzymes, proteins, and DNA that result in cell death. Furthermore, NPs penetrate through the holes of cell wall of microorganisms [60]. NPs also cause lipid peroxidation and depletion fungal membrane ergosterol contents [61]. Higher ratios of surface-to-volume allow NPs to adhere the fungal cell surface, penetrate directly into cell, and cause damage of cell wall [62]. In the past, it has been reported that mycosynthesized iron oxide nanoparticles can prevent apple brown rot [46]. Green iron oxide nanoparticles prevented cherry fruit rot [40]. Citrus brown rot was prevented by bio-fabricated iron oxide nanoparticles [39].

This study has described a simple, predictable, and ecologically secure technique of preventing fruit rot disease of loquat by using green iron oxide nanoparticles. It has been concluded that the synthesized Fe_2O_3 NPs show effective antifungal properties The outcomes showed that rot disease loquat could be effectively controlled by using the optimal concentration of Fe_2O_3 NPs (1.0 mg/ml).

Author contribution F.N. conducted all experiments, collected data, and wrote up the manuscript; M.A. compiled and organized the data; U.H. supervised the isolation of strains; F. and A.K. helped in the characterization of nanoparticles, T.R. and F.A. assisted in antifungal activity analyses, R.N. assisted in field experiments, H.J.C. supervised the write-up, and M.F.H.M. designed and supervised the whole study. All authors have read and agreed to the published version of the manuscript.

Funding This work was financially supported by Higher Education Commission (HEC), Pakistan, under NRPU project No: 9739/Federal/NRPU/R&D/HEC/2017. The authors acknowledge the support from Princess Nourah bint Abdulrahman University Researchers Supporting Project Number (PNURSP2022R15), Princess Nourah bint Abdulrahman University, Riyadh, Saudi Arabia.

Data availability Not applicable

Code availability Not applicable

Declarations

Ethics approval and consent to participate Not applicable

Consent for publication Not applicable

Conflict of interest The authors declare no competing interests.

References

1. Badenes ML, Martinez-Calvo J, Llacer G (2000) Analysis of a germplasm collection of loquat (*Eriobotrya japonica* Lindl.). Euphytica 114(3):187–194
2. Li JQ, Hou CX, Luo N, Deng QX, Wang YQ (2006) Direct embyogenesis from anther culture of loquat. In: II International Symposium on Loquat, vol 750, pp 209–214
3. Vilanova S, Badenes ML, Martínez-Calvo J, Llácer G (2001) Analysis of loquat germplasm (*Eriobotrya japonica* Lindl) by RAPD molecular markers. Euphytica 121(1):25–29
4. Razeto B, Reginato G, Rojas S (2003) Chemical thinning of loquat with naphthalene acetic acid. Horttechnology 13(1):128–132
5. Yang Q, Fu Y, Wang Y, Liu L, Li X, Peng S (2018) Identification of 21 novel S-RNase alleles and determination of S-genotypes in 66 loquat (*Eriobotrya*) accessions. Mol Plant Breed 389(5):1–13
6. Zhang W, Zhao X, Sun C, Li X, Chen K (2015) Phenolic composition from different loquat (*Eriobotrya japonica* Lindl.) cultivars grown in China and their antioxidant properties. Molecules 20(1):542–555
7. Lin SQ (2007) World loquat production and research with special reference to China. In: II International Symposium on Loquat, vol 750, pp 37–44
8. Lin S, Huang X, Cuevas J, Janick J (2007) Loquat: an ancient fruit crop with a promising future. Chronica Hort 47(2):12–15
9. Hussain A, Abbasi NA, Hafiz IA, Shakoor A, Naqvi SS (2011) Performance of loquat (*Eriobotrya japonica*) genotypes under agro-ecological conditions of Khyber Pakhtunkhwa province of Pakistan. Int J Agric Biol 13(5):746–750
10. Abbas MF, Naz F, Batool S, Naeem M, Qamar MI (2018) First evidence of Mucor rot infecting loquat (*Eriobotrya japonica* L.) in Pakistan. Mycopath 16(2):81–85
11. Fisher MC, Henk DA, Briggs CJ, Brownstein JS, Madoff LC, McCraw SL, Gurr SJ (2012) Emerging fungal threats to animal, plant and ecosystem health. Nature 484(7393):186–194
12. Damm U, Sun YC, Huang CJ (2020) Colletotrichum eriobotryae sp. nov. and *Colletotrichum nymphaeae*, the anthracnose pathogens of loquat fruit in central Taiwan, and their sensitivity to azoxystrobin. Mycol Prog 19(4):367–380
13. Jeffries P, Dodd J, Jeger MJ, Plumbley RA (1990) The biology and control of *Colletotrichum* species on tropical fruit crops. Plant Pathol 39(3):343–366
14. Sarkar AK (2016) Anthracnose diseases of some common medicinally important fruit plants. J Med Plants Stud 4(3):233–236
15. Naz F, Abbas MF, Rauf CA, Tariq A, Mumtaz A, Irshad G, Shaheen FA, Hassan I (2017) First report of *Colletotrichum gloeosporioides* causing anthracnose on loquat in Pakistan. Plant Dis 101(8):1550–1550
16. Cao S, Zheng Y, Yang Z, Tang S, Jin P, Wang K, Wang X (2008) Effect of methyl jasmonate on the inhibition of *Colletotrichum acutatum* infection in loquat fruit and the possible mechanisms. Postharvest Biol Technol 49(2):301–307

17. Wu D, Zhang DH, Wang CX, Wei Y, Timko MP, Liang GL (2021) First report of *Fusarium solani* species complex causing root rot of loquat (*Eriobotrya japonica*) in China. Plant Dis 105(05):1562
18. Shah MD, Verma KS, Singh K, Kaur R (2010) Morphological, pathological and molecular variability in *Botryodiplodia theobromae* (Botryosphaeriaceae) isolates associated with die-back and bark canker of pear trees in Punjab, India. Genet Mol Res 9(2):1217–1228
19. Tziros GT (2013) Alternaria alternata causes leaf spot and fruit rot on loquat (*Eriobotrya japonica*) in Greece. Australas Plant Dis Notes 8(1):123–124
20. Abbas MF, Naz F, Rauf CA, Mehmood N, Zhang X, Rosli BH, Gleason ML (2017) First report of *Fusarium solani* causing fruit rot of loquat (*Eriobotrya japonica*) in Pakistan. Plant Dis 101(5):839
21. González-Domínguez E, Martins RB, Del Ponte EM, Michereff SJ, García-Jiménez J, Armengol J (2014) Development and validation of a standard area diagram set to aid assessment of severity of loquat scab on fruit. Eur J Plant Pathol 139(2):419–428
22. Sánchez-Torres P, Hinarejos R, Tuset JJ (2009) Characterization and pathogenicity of *Fusicladium eriobotryae*, the fungal pathogen responsible for loquat scab. Plant Dis 93(11):1151–1157
23. Soler E, Martínez-Calvo J, Llácer G, Badenes ML (2006) Loquat in Spain: production and marketing. In: II International Symposium on Loquat, vol 750, pp 45–48
24. Abbas MF, Naz F (2018) First report of *Diplodia seriata* causing fruit rot of loquat in Pakistan. J Plant Pathol 100(2):325–325
25. Naz F, Abbas MF, Rauf CA, Tariq A, Mumtaz A, Irshad G, Shaheen FA, Hassan I (2017) First report of *Colletotrichum gloeosporioides* causing anthracnose on loquat in Pakistan. Plant Dis 101(8):1550–1550
26. Abbas MF, Naz F, Tariq A, Mumtaz A, Irshad G, Rauf CA (2017) First report of *Curvularia lunata* causing leaf spots on loquat from Pakistan. J Plant Pathol 98(2):374–374
27. Abbas MF, Naz F, Rauf CA, Khan MA (2016) Cultural, morphological, pathogenic and molecular characterization of *Alternaria mali* associated with necrotic leaf spot of loquat. Int J Biosci 9:271–228
28. Nasir M, Iqbal B, Saqib M, Sajjad M, Niaz MZ, Idrees M, Abbas W, Mohy-ud-Din G (2016) Evaluation and standardization of fungicides against plant diseases in Punjab-Pakistan crop production system. J Agric Sci (Lahore) 54(2):233–249
29. Ramzy AY, Shakil A, Sabah Z (2021) Pesticide residues in Fish, Karachi-Pakistan: a review. J Agric Environ 5(1):25–29
30. Lo CC (2010) Effect of pesticides on soil microbial community. J Environ Sci Health B 45(5):348–359
31. Conway WS, Leverentz B, Janisiewicz WJ, Blodgett AB, Saftner RA, Camp MJ (2004) Integrating heat treatment, biocontrol and sodium bicarbonate to reduce postharvest decay of apple caused by *Colletotrichum acutatum* and *Penicillium expansum*. Postharvest Biol Technol 34(1):11–20
32. Ragsdale NN, Sisler HD (1994) Social and political implications of managing plant diseases with decreased availability of fungicides in the United States. Annu Rev Phytopathol 32(1):545–557
33. Azizbekyan RR (2013) Use of spore-forming bacteria as biological plant protection products. Biotechnol 1:69–77
34. Khakimov AA, Omonlikov AU, Utaganov SBU (2020) Current status and prospects of the use of biofungicides against plant diseases. GSC Biol Pharm Sci 13(3):119–126
35. Elmer W, White JC (2018) The future of nanotechnology in plant pathology. Annu Rev Phytopathol 56:111–133
36. Narayanan KB, Sakthivel N (2011) Green synthesis of biogenic metal nanoparticles by terrestrial and aquatic phototrophic and heterotrophic eukaryotes and biocompatible agents. Adv Colloid Interface Sci 169(2):59–79
37. Murad MT, Habib A, Ashraf W, Rehman MS, Rafiq F, Murad S, Zeshan MA (2021) Efficacy of desert medicinal plants against postharvest losses caused by *Botrytis cineria* (Pers.) in strawberry. Plant Prot 5(1):31–38
38. Wang T, Jin X, Chen Z, Megharaj M, Naidu R (2014) Green synthesis of Fe nanoparticles using *Eucalyptus* leaf extracts for treatment of eutrophic wastewater. Sci Total Environ 466:210–213
39. Ali M, Haroon U, Khizar M, Chaudhary HJ, Munis MFH (2020) Facile single step preparations of phyto-nanoparticles of iron in *Calotropis procera* leaf extract to evaluate their antifungal potential against *Alternaria alternata*. Curr Plant Biol 23:100157
40. Zubair MS, Munis MFH, Alsudays IM, Alamer KH, Haroon U, Kamal A, Attia H (2022) First report of fruit rot of cherry and its control using Fe_2O_3 nanoparticles synthesized in *Calotropis procera*. Molecules *27*(14):4461
41. Kour A, Shawl AS, Rehman S, Sultan P, Qazi PH, Suden P, Rk K, Verma V (2008) Isolation and identification of an endophytic strain of *Fusarium oxysporum* producing podophyllotoxin from *Juniperus recurva*. World J Microbiol Biotechnol 24(7):1115–1121
42. Tafinta IY, Shehu K, Abdulganiyyu H, Rabe AM, Usman A (2013) Isolation and identification of fungi associated with the spoilage of sweet orange (*Citrus sinensis*) fruits in Sokoto State. Nig J Basic Appl Sci 21(3):193–196
43. Koh RBL, Barbosa CFC, Aquino VM, Galvez LC (2021) Extraction of high molecular weight DNA suitable for next-generation sequencing from the fiber crop abaca. Ind Crops Prod 161:113194
44. White TJ, Bruns T, Lee SJWT, Taylor J (1990) Amplification and direct sequencing of fungal ribosomal RNA genes for phylogenetics. PCR Protocols 18(1):315–322
45. Kumar S, Stecher G, Tamura K (2016) MEGA7: molecular evolutionary genetics analysis version 7.0 for bigger datasets. Mol Biol Evol 33(7):1870–1874
46. Akbar M, Haroon U, Ali M, Tahir K, Chaudhary HJ, Munis MFH (2022) Mycosynthesized Fe_2O_3 nanoparticles diminish brown rot of apple whilst maintaining composition and pertinent organoleptic properties. J Appl Microbiol *132*(5):3735–3745
47. Yassin MT, Mostafa AAF, Al-Askar AA (2021) In vitro antagonistic activity of *Trichoderma harzianum* and *Trichoderma viride* strains compared to carbendazim fungicide against the fungal phytopathogens of *Sorghum bicolor* (L.). Moench J Biol Pest Control 31(1):1–9
48. Iliger KS, Sofi TA, Bhat NA, Ahanger FA, Sekhar JC, Elhendi AZ, AL-Huqail AA, Khan F (2021) Copper nanoparticles: green synthesis and managing fruit rot disease of chilli caused by *Colletotrichum capsici*. Saudi J Biol Sci 28(2):1477– 1486.
49. Malik P, Shankar R, Malik V, Sharma N, Mukherjee TK (2014) Green chemistry based benign routes for nanoparticle synthesis. J Nanopart 3:1–14
50. Hafizi R, Salleh B, Latiffah Z (2013) Morphological and molecular characterization of *Fusarium solani* and *Fusarium oxysporum* associated with crown disease of oil palm. Braz J Microbiol 44:959–968
51. Alghuthaymi MA, Ali AA, Hashim AF, Abd-Elsalam KA (2016) A rapid method for the detection of *Ralstonia solanacearum* by isolation DNA from infested potato tubers based on magnetic nanotools. Philiph Agric Scientist 99(1):113–118
52. Mohanpuria P, Rana NK, Yadav SK (2008) Biosynthesis of nanoparticles: technological concepts and future applications. J Nanopart Res 10(3):507–517
53. Ahmed J, Ali M, Sheikh HM, Al-Kattan MO, Haroon U, Safaeishakib M, Munis MFH (2022) Biocontrol of fruit rot of Litchi chinensis using zinc oxide nanoparticles synthesized in *Azadirachta indica*. Micromach 13(9):1461

54. Yim HS, Chye FY, Rao V, Low JY, Matanjun P, How SE, Ho CW (2013) Optimization of extraction time and temperature on antioxidant activity of *Schizophyllum commune* aqueous extract using response surface methodology. J Food Sci Technol 50(2):275–283
55. Bae E, Lee BC, Kim Y, Choi K, Yi J (2013) Effect of agglomeration of silver nanoparticle on nanotoxicity depression. Kor J Chem Eng 30(2):364–368
56. Mohamed YM, Azzam AM, Amin BH, Safwat NA (2015) Mycosynthesis of iron nanoparticles by *Alternaria alternata* and its antibacterial activity. Afr J Biotechnol 14(14):1234–1241
57. Zakariya NA, Majeed S, Jusof WHW (2022) Investigation of antioxidant and antibacterial activity of iron oxide nanoparticles (IONPS) synthesized from the aqueous extract of *Penicillium spp*. Sensors Int 3:100164
58. Bhuiyan MSH, Miah MY, Paul SC, Aka TD, Saha O, Rahaman MM, Ashaduzzaman M (2020) Green synthesis of iron oxide nanoparticle using *Carica papaya* leaf extract: application for photocatalytic degradation of remazol yellow RR dye and antibacterial activity. Heliyon 6(8):e04603
59. Lemire JA, Harrison JJ, Turner RJ (2013) Antimicrobial activity of metals: mechanisms, molecular targets and applications. Nat Rev Microbiol 11(6):371–384
60. Alghuthaymi MA, Almoammar H, Rai M, Said-Galiev E, Abd-Elsalam KA (2015) Myconanoparticles: synthesis and their role in phytopathogens management. Biotechnol Biotechnol Equip 29(2):221–236
61. Senthilkumar SR, Sivakumar T (2014) Green tea (*Camellia sinensis*) mediated synthesis of zinc oxide (ZnO) nanoparticles and studies on their antimicrobial activities. Int J Pharm Pharm Sci 6(6):461–465
62. Xie Y, He Y, Irwin PL, Jin T, Shi X (2011) Antibacterial activity and mechanism of action of zinc oxide nanoparticles against (*Campylobacter jejuni*). Appl Environ Microbiol 77(7):2325–2331